European Journal of Medicinal Chemistry 223 (2021) 113638

Contents lists available at ScienceDirect

European Journal of Medicinal Chemistry

journal homepage: http://www.elsevier.com/locate/ejmech

Design, synthesis, biological evaluation and structural characterization of novel GEBR library PDE4D inhibitors

Chiara Brullo [a], Federica Rapetti [a], Sara Abbate [b], Tommaso Prosdocimi [b], Archimede Torretta [b], Marta Semrau [c], Matteo Massa [a], Silvana Alfei [a], Paola Storici [c], Emilio Parisini [b, d, *], Olga Bruno [a, **]

[a] Department of Pharmacy, School of Medical and Pharmaceutical Sciences, University of Genova, Viale Benedetto XV 3, 16132, Genova, Italy
[b] Center for Nano Science and Technology @ PoliMi, Istituto Italiano di Tecnologia, via Giovanni Pascoli 70/3, 20133, Milano, Italy
[c] Elettra Sincrotrone Trieste S.C.p.A., SS 14 - km 163,5 in AREA Science Park, 34149, Trieste, Italy
[d] Latvian Institute of Organic Synthesis, Aizkraukles 21, LV, 1006, Riga, Latvia

ARTICLE INFO

Article history:
Received 16 March 2021
Received in revised form
7 June 2021
Accepted 8 June 2021
Available online 13 June 2021

Keywords:
PDE4D
GEBR library
PDE4D inhibitors
Crystallographic structure
NMR studies

ABSTRACT

Memory and cognitive functions depend on the cerebral levels of cyclic adenosine monophosphate (cAMP), which are regulated by the phosphodiesterase 4 (PDE4) family of enzymes. Selected rolipram-related PDE4 inhibitors, members of the GEBR library, have been shown to increase hippocampal cAMP levels, providing pro-cognitive benefits with a safe pharmacological profile. In a recent SAR investigation involving a subset of GEBR library compounds, we have demonstrated that, depending on length and flexibility, ligands can either adopt a twisted, an extended or a protruding conformation, the latter allowing the ligand to form stabilizing contacts with the regulatory domain of the enzyme. Here, based on those findings, we describe further chemical modifications of the protruding subset of GEBR library inhibitors and their effects on ligand conformation and potency. In particular, we demonstrate that the insertion of a methyl group in the flexible linker region connecting the catechol portion and the basic end of the molecules enhances the ability of the ligand to interact with both the catalytic and the regulatory domains of the enzyme.

1. Introduction

Alzheimer's disease (AD) is a widespread age-related neurodegenerative disorder that drastically impairs cognitive abilities and memory functions, thus imposing a heavy physical, emotional and economic burden on patients and their families. To date, there is no effective cure for AD. Physiological intracellular levels of the second messenger cyclic adenosine monophosphate (cAMP) are known to be crucially involved in sustaining correct memory functions [1]. Such levels are regulated by the phosphodiesterase 4 (PDE4) family of enzymes, which catalyze the hydrolysis of cAMP to 5′-AMP. In recent years, a number of PDE4 inhibitors have been shown to effectively improve memory and cognitive functions in AD patients [2,3]. Indeed, by reducing excessive cAMP hydrolysis, the inhibition of phosphodiesterase 4 (PDE4) enzymes increases hippocampal cAMP levels, potentiates the cAMP cascade and triggers the activation of transcription factors that regulate the expression of central nervous system (CNS) genes connected to memory and to learning processes. Of all the different existing PDE4 isoforms, PDE4B and PDE4D are widely considered as the two best targets for the treatment of cognition deficit, anxiety, depression and other neuropsychological conditions. Whereas PDE4B inhibition provides antidepressant-like effects, the pharmacological profile of PDE4D inhibitors is more related to cognition improvement [4]. Interestingly, the role of PDE4D in cognition has been further validated in the context of the genetic disorder acrodysostosis, a rare congenital malformation syndrome that causes mental retardation, brachydactyly and facial dysplasia. Such disorder originates from PDE4D missense mutations that are likely to impair the regulation mechanism of the enzyme [5–7]. PDE4 systemic inhibition has always been associated with severe side effects such as emesis and diarrhea. Considering the existence of several PDE4 sub-types (A to D), each of them produced as several splicing variant isoforms of

* Corresponding author. Center for Nano Science and Technology @ PoliMi, Istituto Italiano di Tecnologia, Via G. Pascoli 70/3, 20133, Milano, Italy.
** Corresponding author.
E-mail addresses: emilio.parisini@osi.lv (E. Parisini), obruno@unige.it (O. Bruno).

https://doi.org/10.1016/j.ejmech.2021.113638
0223-5234/

different length, the development of isoform specific drugs is generally regarded as a viable option for the design of safer inhibitors [8]. In their seminal work, Burgin and coworkers demonstrated that it is possible to exploit the stabilization of the UCR2 regulatory domain over the entrance of the catalytic pocket to selectively target the PDE4D/B long isoforms [5,9,10].

The GEBR library is an established and well-known panel of catechol-based PDE4 inhibitors. The members of this library feature three general moieties (Fig. 1): 1) the catechol portion. Since the development of rolipram, this scaffold has been one of the most investigated in PDE4 drug development studies. In all the GEBR library compounds, one of the hydroxy catechol moiety is substituted with a cyclopentyl group, which interacts with the Q2 pocket of the enzyme's catalytic domain; the other, the Q1-directed catechol substituent, is either a methoxy or a difluoromethoxy group, the latter having been introduced with the expansion of the library in 2015 [11]. 2) the linker region. This is the most variable portion of the entire library. Indeed, we extensively modified the chemical nature of the linker in order to explore how different functionalities may result in the possible exploration of the M-pocket. Six families of linkers have been developed within the GEBR library, each comprising up to 10 members featuring alternative chemical modifications [12,13]. 3) the basic end. All of the more active compounds feature a morpholine, a dimethylmorpholine or 4-hydroxypiperidine as the terminal portion.

Several members of the GEBR library (particularly GEBR-7b [12], GEBR-54 [13] and GEBR-32a [14], Fig. 2) showed interesting PDE4D3 selective inhibition, and *in vitro* and *in vivo* assays evidenced their great potential as therapeutic agents in pathologies characterized by a dysregulation of memory and cognitive performance, such as Alzheimer's disease. Moreover, unlike other PDE4 inhibitors, these compounds showed only limited side-effects such as sedation or emesis when tested in animal models [13–15].

To contribute to the elucidation of the molecular bases of selective inhibition, we recently provided a structural and functional characterization of several members of the GEBR family, leading to the identification of three major ligand conformational classes, which we classified as protruding, twisted, and extended [16]. Interestingly, our X-ray crystallography study highlighted the ability of the protruding compounds to explore the S-pocket, pointing towards the external portion of the catalytic cavity, in the proximity of the area that in long isoforms is occupied by the UCR2 helix. This structural property is quite innovative for PDE4 inhibitors, as only a few other recently developed compounds have been shown to be able to exploit this space [5]. Also, on the basis of molecular dynamic simulations we postulated hydrophobic interactions between the tail portion of the ligand and the capping portion of the enzyme (Phe196). In addition, pharmacological analyses showed that the shorter compounds (such as GEBR-7b and its fluorinated analogue GEBR-20b, Fig. 2) do not inhibit

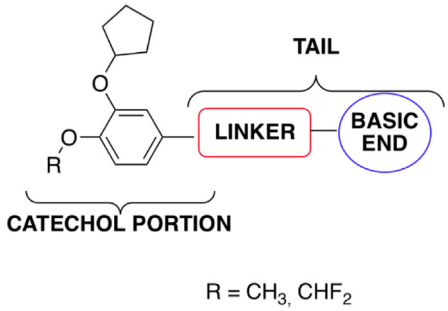

Fig. 1. General structure of GEBR library compounds.

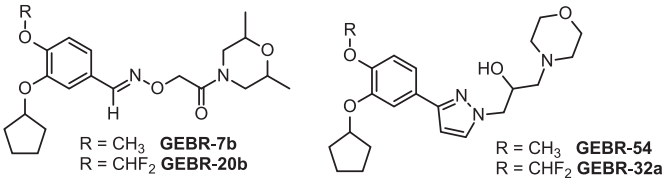

Fig. 2. Structures of memory enhancers GEBR-7b, GEBR-20b, GEBR-54 and GEBR-32a.

differentially the PDE4 catalytic domain and the full-length PDE4D3, while with the lengthening and the enhanced flexibility of the tail (GEBR-4a and GEBR-11b, Fig. 3) [16] a differential behavior starts to appear. More recently, enantiomeric separation was performed on lead GEBR-32a and IC_{50} values against both the PDE4D catalytic domain and the long PDE4D3 isoform were determined for both enantiomers [17]. The (*S*)-enantiomer was more active than the (*R*)-configured one when measured against the full-length protein, whereas this fold-difference was reduced when measured against the catalytic domain. These data clearly showed that the inhibitory activity of GEBR-32a is significantly influenced by the configuration of the stereogenic center and confirmed our hypothesis that the tail portion of GEBR-32a contributes significantly to the inhibition of the full-length PDE4D enzyme.

Altogether, these results suggested that longer and more flexible chains might efficiently adapt to the chemical environment of the active site, in particular when a regulatory domain of the enzyme is capping the catalytic pocket. Based on these data, the subset of protruding ligands appeared to be the most promising candidate for further library development.

To enhance the ability of the ligand to interact with the regulatory capping portion of the enzyme, we designed and synthesized a new series of compounds featuring the catechol portion, an unmodified basic end, and a flexible linker region bearing an additional methyl group (compounds type A, Fig. 4). Based on our previous SAR study on GEBR library inhibitors, we hypothesized that a ligand chemical derivatization strategy could be adopted to provide stabilizing hydrophobic interactions with the surrounding residues, either downwards towards the bottom of the catalytic pocket or upwards towards the capping helix. To this end, the introduction of a methyl group on the linker appeared to be appropriate and potentially effective given the availability of free space and the nonpolar nature of the surrounding region. Indeed, it is well known that methyl group can exert electronic and steric effects on biologically active molecules leading to increase potency and selectivity towards the target, or to enhance resistance to metabolic transformation, as the numerous examples in the history of medicinal chemistry demonstrate [18].

In addition, in order to confirm that a certain flexibility in the chain is required to better interact within the catalytic pocket as well as with the UCR2 portion, we designed and synthesized a second group of compounds (type B, Fig. 4). In these constrained derivatives, the methyl group is entered in a five membered cycle condensed with the phenyl of the catechol moiety.

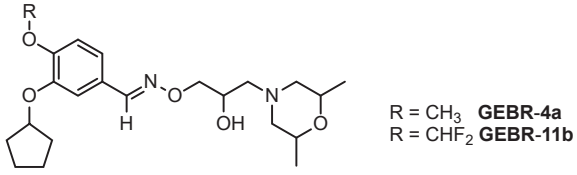

Fig. 3. The more flexible GEBR-4a and its fluorinated analogue GEBR-11b

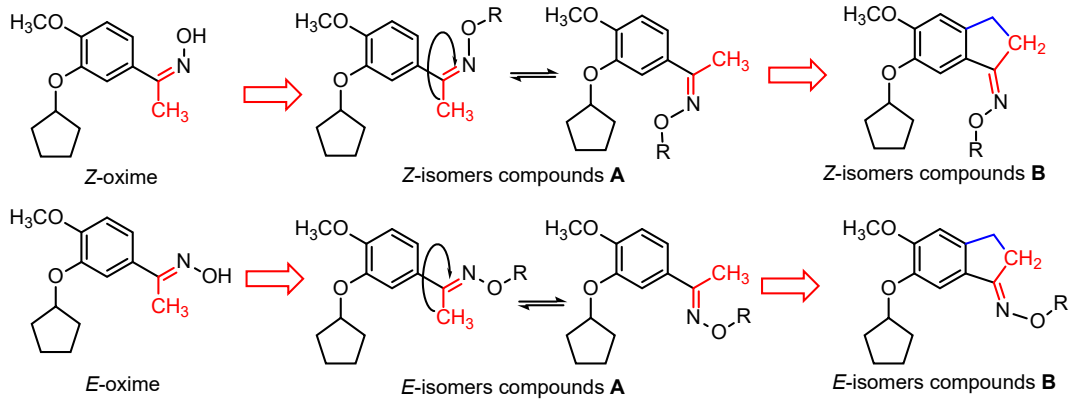

Fig. 4. Design of new compounds type A and B.

Since the key intermediates for the synthesis of compounds A and B are ketoximes that could be obtained in both conformation *E*/*Z* (Fig. 4), we firstly hypothesized to obtain for each derivatives a mixture of two isomers, as previously reported for similar compounds [12]. In constrained compounds type B, by blocking the methyl in the condensed cycle with the phenyl we would force the chain to assume two different arrangements in space, one in which the terminal amine is closer to the catechol ring (*Z* isomers) and another in which it is further away (*E* isomers).

However, as shown in Table 1 and discussed in the following chemistry section, type A compounds actually afforded only Z isomers while type B compounds afforded only *E* isomers.

We evaluated the percentage inhibition of the PDE4D catalytic domain for all the synthesized compounds at 100 μM concentration. Based on these end-point assays, we then obtained dose dependent curves and measured the IC_{50} values against both the PDE4D catalytic domain alone and the PDE4D3 isoform only for those compounds showing >50% inhibition. Finally, we carried out the X-ray crystallographic characterization of the complexes between the PDE4D catalytic domain and the most active inhibitors, two of which (compounds **1b** and **2a**) will be discussed here in detail.

2. Results and discussion

2.1. Chemistry

The new methyl derivatives compounds **1**, **2** and **3** were synthetized starting from 3-cyclopentyloxy-4-methoxybenzaldehyde **6** (Scheme 1) [19], which was reacted with the suitable Grignard reagent to obtain the 1-[3-(cyclopentyloxy)-4-methoxyphenyl] ethanol **7**. The subsequent oxidation to methylketone **8** was performed with pyridinchlorochromate (PCC) in cyclohexane; despite compounds **7** and **8** are already reported in the literature [20,21], we have optimized both the methods and reaction yields. Then, the intermediate ketone **8** was transformed in the corresponding oxime derivative **9**; this compound also was already reported in two patents, but the configuration of the C=N bond was never assigned [22,23]. Therefore, we performed an in-depth analysis of the ^{1}H NMR and ^{13}C NMR spectra and assigned the Z configuration to the C=N bond (see Supporting Material).

Generally, a mixture of two *Z*/*E* isomers is obtained. Therefore, in the ^{13}C NMR spectra two signals very close together in the range 150–160 ppm and belonging to the oxime carbon atom (C=N) can be observed and can be used to assign the exact configurations. In particular, according to literature [24], the signal with higher chemical shift belongs to the oxime carbon of the *E* form, while that observed at lower δ values results from the *Z* isomer. In this study, unlike other previously synthesized oxime derivatives, which were obtained as *E*/*Z* mixtures [12], **9** was obtained as a single compound; hence, comparative analyses between the chemical shift of the carbon atoms of the oxime group was not possible. On the other hand, since the difference between the δ values of the C=N signals of the two isomers is generally minimal, the configuration of the single compound could not be assigned with certainty on the basis of the chemical shift of its C=N group only. The configuration of the C=N bond was therefore assigned on the basis of the methyl chemical shift (2.27 ppm) in the ^{1}H NMR spectrum, according to what previously reported for the *E* (2.19 ppm) and Z (2.26 ppm) isomers of acetophenone oxime derivatives [25]. In addition, in the ^{13}C NMR analyses, the CH_3 signal was observed at δ values corresponding to those reported for analogues *Z* isomers [24], thus confirming our hypothesis.

The synthesis of compounds **1a**–**c** and **2a**,**b** involved the treatment of the oxime **9** with the suitable chloroacetyl- or chlropropionyl-amides [13], in anhydrous DMF, in the presence of anhydrous K_2CO_3 (for **1a**,**b**), sodium ethoxide (for **1c)** or NaH (60% dispersion in mineral oil) (for **2a**,**b**) (Scheme 1). The oxime **9** was then treated with epichlorohydrin in sodium ethoxide to obtain (1*Z*)-1-[3-(cyclopentyloxy)-4-methoxyphenyl]ethanone-*O*-(oxiran-2ylmethyl)-oxime **10**, which in turn was reacted with excess of morpholine or 2,6-dimethylmorpholine (for **3a,b**) or with piperidin-1-ol in anhydrous DMF (for **3c**) (Scheme 1).

To obtain compounds **4** and **5**, *trans*-ferulic acid **11** was firstly reduced to 3-(4-hydroxy-3-methoxyphenyl) propanoic acid **12** [26] (Scheme 2) using H-cube hydrogenator. The treatment of **12** with methansulfonic acid yielded the indanone **13** [27], which was then alkylated with cyclopentyl bromide in the presence of K_2CO_3 to give 6-(cyclopentyloxy)-5-methoxindan-1-one **14**. The subsequent reaction of the ketone group with hydroxylamine hydrochloride in ethanol led to the corresponding oxime **15**. The 1H NMR and 13C spectra analysis enabled us to assign the *E* configuration to the C=N bond of compound **15**. In this regard, the chemical shift of the signal belonging to the carbon atom of the C=N group in the 13C NMR spectrum (164 ppm, see Supporting Material) was discriminant. According to what reported for similar oximes [28], *E* isomers provide signals at δ values greater than 160, while *Z* ones at values lower than 160.

Derivatives **4a**–**c** were obtained by reacting oxime **15** with the proper chloroacetyl amides [13] in the presence of anhydrous K_2CO_3 in anhydrous DMF. Moreover, to obtain derivatives **5a**–**c**, oxime **15** was converted in the corresponding oxirane **16** by reaction with epichlorohydrin in absolute ethanol in the presence of sodium ethoxide. Then, the latter was reacted with excess

Table 1
Structures of the new series compounds 1a–c, 2a–b, 3a–c, 4a–c and 5a–c.

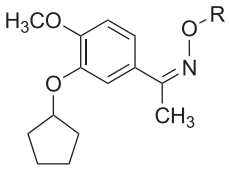

A: 1a–c; 2a,b; 3a–c

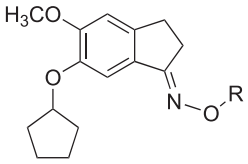

B: 4a–c; 5a–c

Comp.	Type	R	—N
1a	A	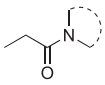	
1b	A	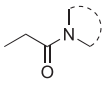	
1c	A	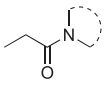	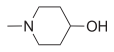
2a	A	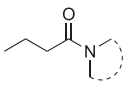	
2b	A	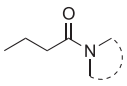	
3a	A	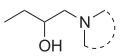	
3b	A	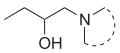	
3c	A	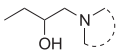	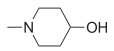
4a	B	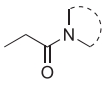	
4b	B	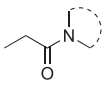	
4c	B	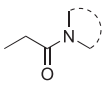	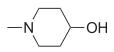
5a	B	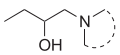	
5b	B	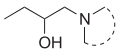	
5c	B	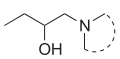	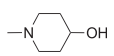

morpholine or 2,6-dimethylmorpholine to give **5a**,**b** or with piperidin-1-ol in anhydrous DMF to obtain **2c** (Scheme 2).

2.2. Enzymatic assays and SAR considerations

Based on preliminary end-point assays carried out on the PDE4D catalytic domain with each of the newly synthesized species at 100 μM concentration, compounds **1c, 3c, 4a-c** and **5a-c** did not show significant inhibitory activity (inhibition <30% in all cases), hence we classified them as inactive.

For compounds **1a-b**, **2a-b** and **3a-b**, the inhibitory activity was measured against both the catalytic domain only and against the PDE4D3 isoform. Results expressed as IC_{50} (μM) values are reported in Table 2, while the full set of the corresponding dose-response curves are shown in Fig. 5. In all cases, a significant increase in IC_{50} can be observed in going from the catalytic domain to the PDE4D3 isoform, suggesting that contacts with the inhibitory domain capping the entrance of the catalytic pocket are formed. Interestingly, within the whole series, compounds **1a** and **1b** show the lowest IC_{50} values, while, at the same time, also featuring a sizeable (5–15-fold) decrease in IC_{50} in going from the catalytic domain to the full length enzyme. Moreover, it is worth noting that compound **1b** is the methylated equivalent of GEBR-7b, whose IC_{50} we measured previously (16 ± 2 and 11 ± 2 μM against the catalytic domain and the full length enzyme, respectively) [16]. The decrease in IC_{50} suggests that the introduction of a methyl group in the linker region has improved significantly the overall potency of the compound, confirming our hypothesis formulated in the series design. Indeed, the methylation increased lipophilicity enhancing the interaction of the linker with the catalytic domain, as confirmed by X-ray crystallography. The presence of a morpholine instead of a dimethylmorpholine in the tail end does not affect significantly the potency of the ligand (see compound **1a).**

An outlier in the list is represented by compound **2a**, whose IC_{50} far exceeds those of the remaining compounds in the series. Compounds series **2**, which relative to **1** features a one extra carbon atom in the chain connecting the morpholine ring and the catechol moiety, are predicted to be more flexible; hence, they are in principle capable of adopting a wider spectrum of conformations within the catalytic pocket. Indeed, this is confirmed by X-ray crystallography analysis of **2a**, which provides evidence of two alternate conformations in the catalytic pocket, one of them featuring an unfavorable twisted arrangement, as we discuss more carefully in section *2.3.* Compound **2b**, on the contrary, showed potency in the same range observed for compounds **1** and **3**. We can suppose that, owing to steric hindrance, the dimethylmorpholine ring, in this case, prevents the twisted arrangement and therefore **2b** should assume only the most efficient protruding conformation.

As concerns the inactive derivatives, both compounds **1c** and **3c** are characterized by the presence of 4-hydroxypiperidine moiety in the terminal end of the tail. To justify their poor ability to inhibit both forms of enzyme (PDE4D cat and full PDE4D3), we can hypothesize that the polarity of the hydroxy group is detrimental for a good interaction with the hydrophobic part of the catalytic domain as well as with the capping domain at the entrance of the catalytic pocket. The same considerations can be extended to compounds **3a** and **3b,** which, bearing the hydroxy substituent in the chain, showed a lower potency in comparison with linear compounds **1a** and **1b**.

Finally, all the more rigid compounds **4** and **5** resulted to be inactive, thus confirming that the tail flexibility is an essential feature for GEBR-library molecules to enter the catalytic pocket, settle on its hydrophobic floor and reach out towards the regulatory domain and interact with it.

2.3. Crystallographic studies

The PDE active site, which is highly conserved across the different isoforms of the enzyme, features three distinct portions: a metal binding pocket (M), hosting two octahedrally-coordinated metal ions (Zn and Mg), the so-called Q switch and P clamp pocket (Q), where the residues Ile502 and Phe538 provide a tight

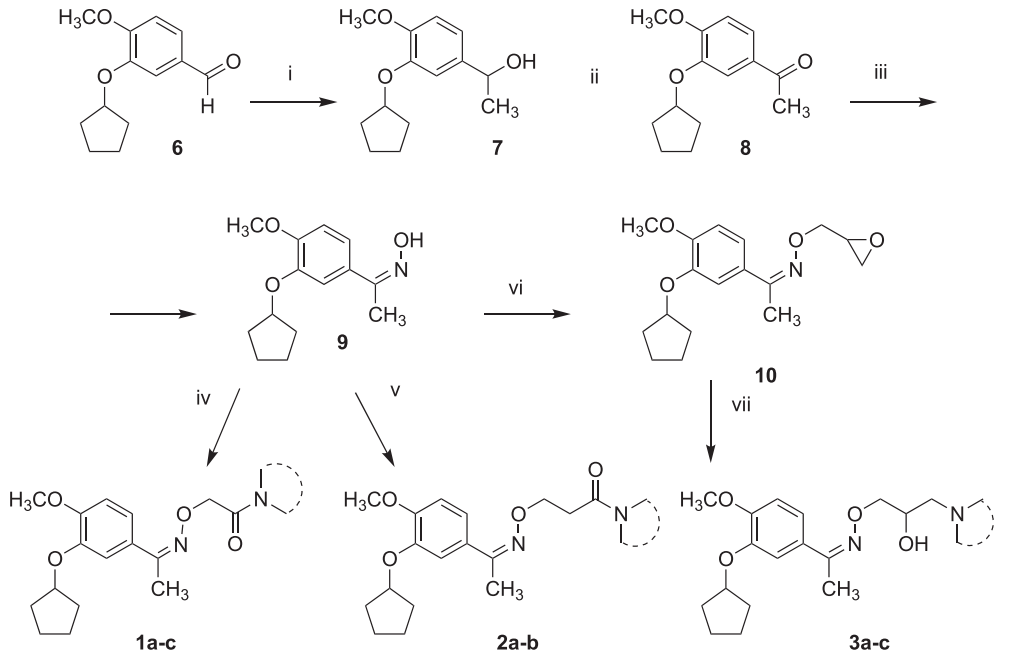

Scheme 1. Synthesis of derivatives **1a**–**c**, **2a,b**, **3a**–**c**. Reagents and conditions: (i) Mg/I_2, an. Et_2O, CH_3I, 30–40 °C, 3h, 100%. (ii) Pyridinium chlorochromate, cyclohexane, 70 °C, 3 h, 94%. (iii) $NH_2OH.HCl$, $NaHCO_3$, EtOH, 60 °C, 4 h, 63%. (iv) K_2CO_3, proper chloroacetylamide, an. DMF, 60 °C, 18 h, (**1a**,**b**) or EtONa, 1-(chloroacetyl)piperidin-4-ol, an. DMF, 50–60 °C, 24 h (**1c**), 41–87%. (v) NaH, an. DMF, 0 °C, 2 h, proper chloropropionylamide, rt, 18 h, 24–56%. (vi) epichlorohydrin, EtONa, DMF, 50–60 °C, 12 h, 53%. (vii) morpholine or 2,6-dimethylmorpholine, 50–60 °C, 18 h (**3a,b**) or piperidin-1-ol, an. DMF, 60 °C, 18 h (**3c**), 34–96%.

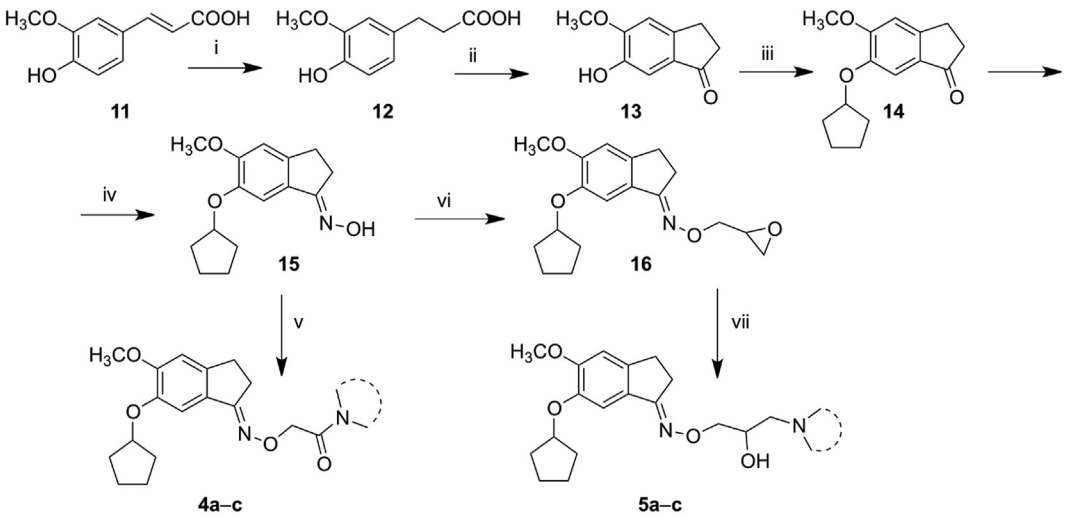

Scheme 2. Synthesis of derivatives **4a**–**c** and **5a**–**c**. Reagents and conditions: (i) full-H_2 mode, CH_3OH, Pd/C 5%, flow 1 mL/min rt, quantitative yield. (ii) CH_3SO_3H, N_2, 90 °C, 10 min, 56%. (iii) bromocyclopentane, K_2CO_3, KI, an. DMF, 65 °C, 22 h, 73%. (iv) $NH_2OH.HCl$, $NaHCO_3$, EtOH, 60 °C, 2 h, 59%. (v) K_2CO_3, proper chloroacetylamide, an. DMF, 50–60 °C, 18 h, 33–100%. (vi) epichlorohydrin, an. DMF, 40–50 °C, 18 h, 50%. (vii) morpholine or 2,6-dimethylmorpholine, 50–60 °C, 18h (**5a,b**) or piperdin-1-ol, an. DMF, 50–60 °C, 18 h (**5c**), 41–46%.

cAMP-stabilizing environment, and a solvent-filled pocket (S). All catechol-based inhibitors known to date are invariably stabilized in the active site by the same crucial interaction of the P-clamp (Ile502 and Phe538) with the aromatic ring of the catechol shown by the rolipram complex (PDB code: 1OYN) and by further, mostly water-mediated, interactions within the M, the Q and the S portions of the catalytic pocket. In a SAR investigation involving different members of the GEBR library of rolipram-related PDE4 inhibitors, we have previously demonstrated that in a selected pool of inhibitors, a large conformational variability can be observed at the level of the tail, which, depending on length and flexibility, can take a protruding, a twisted or an extended conformation [16].

Based on our previous study, we identified the protruding compounds as the most promising candidates for the development of the next generation of GEBR compounds. Indeed, they feature a tail that develops within the S pocket of the catalytic site, a region where the ligand can interact with the UCR2 of the enzyme, thus achieving further stabilization and an enhanced specificity for long PDE4D isoforms.

Within the GEBR library, the subset of ligands featuring a linear scaffold were found to adopt a protruding conformation and were therefore selected for subsequent optimization.

Table 2
Inhibitory activity on PDE4 catalytic domain and full-length PDE4D3 enzyme of compounds **1a**–**c**, **2a**, **2b**, **3a**–**c**.

Compounds	IC_{50} μM[a] PDE4D Cat	IC_{50} μM[a] PDE4D3
1a	2.8 ± 0.1	0.16 ± 0.01
1b	2.5 ± 0.2	0.47 ± 0.02
1c	Inactive	
2a	33.1 ± 4.6	11.2 ± 0.6
2b	4.6 ± 0.5	3.6 ± 0.3
3a	6.9 ± 0.7	0.72 ± 0.05
3b	4.1 ± 0.2	1.1 ± 0.8
3c	Inactive	

[a] IC_{50} values were obtained by plotting dose-response curves against the catalytic domain only (PDE4D Cat) and against the PDE4D3 isoform. The reported data are the mean values of three replicates ± SD (standard deviation).

In particular, in the new ligands reported here we enhanced the hydrophobicity by adding a methyl group on the first carbon atom after the aromatic ring of the catechol. In linear compounds, the hydrogen of the first sp2 carbon atom of the linker points towards the highly solvated bottom of the catalytic pocket. Given the length and the flexibility of the tail, we hypothesized that the introduction of a hydrophobic methyl group in the chain would allow a rotation of the sp2 carbon to favor an upward orientation of the methyl and provide further stabilization energy by interacting with Phe196. This would also allow the rest of the flexible tail to maintain a protruding conformation and force the following N and O atoms to lay over the solvation sphere of the metal ions. However, the crystal structure of the complex between compound **1b** (named as GEBR-41b in the GEBR library) and the PDE4D catalytic domain reveals that the methyl group actually points towards the bottom of the catalytic pocket, forming stabilizing van der Waals interactions with residues Tyr159, Met273, Leu319, Ile336 and Phe340 near the metal binding pocket (Fig. 6A and B).

Unlike with compound **1b**, where the ligand is completely protruding, the crystal structure of the complex with compound **2b** (GEBR-42a) shows that in one of the two independent crystallographic monomers the ligand assumes a protruding conformation, while in the other a twisted conformation. In both monomers, the methyl group of **2b** point toward the region of the Q portion containing Met273, Leu319 and Phe372, where stabilizing van der Waals interactions take place. However, relative to compound **1b**, the methyl group moves away from the underlying hydrophilic metal binding region, as shown by Fig. 7. Interestingly, while the protruding conformation of **2b** is very similar to that of **1b**, its twisted conformation features a van der Waals contact between the morpholine moiety and the methyl group in the linker. Here, the methyl group is rotated by approximately 90° compared to the methyl group in compound **1b** and lies almost parallel to the underlying solvated region of the metal binding site.

Data collection and statistical analyses are reported in Table 3.

3. Conclusions

As we demonstrated in our previous SAR study, rolipram-related GEBR-library compounds featuring a flexible tail that protrudes from the catalytic pocket are capable of interacting with the UCR2 regulatory portion of the enzyme in long PDE4D isoforms. Hence, they are promising candidates for further drug development studies aiming at reducing the side effects that are usually associated with PDE4 inhibition. Here, starting from a GEBR-library subset of protruding PDE4D inhibitors, we chemically modified the linker region of the compounds *via* the introduction of a methyl group, with the aim to enhance the interaction of the linker portion of the compounds with the hydrophobic residues that are in its proximity. Indeed, in the case of **1b** (GEBR-41b), we have shown that the methyl group interacts with hydrophobic residues in the Q region and provides further stabilization energy to the ligand in its protruding conformation inside the catalytic pocket. However, in the crystal structure, the one-carbon longer tail of **2a** (GEBR-42a) displays two alternative conformations in the two independent catalytic domain-ligand complexes in the dimer, a protruding and a twisted conformation, the former resembling GEBR-41b while the latter featuring van der Waals interactions between the morpholine moiety and the methyl group in the linker region. Hence, owing to its enhanced flexibility, **2a** can feature a twisted conformation that reduces the interactions with the capping portion of the regulatory domain, thus substantially reducing the overall potency of the ligand.

As previously reported, the reaction between 6-(cyclopentyloxy)-5-methoxindan-1-one and hydroxylamine gave only *E*-oxime derivative, and therefore only *E*-isomers of series **4** and **5**. Thus, it was not possible to verify the entire hypothesis formulated in the molecules design of constrained derivatives. On the other hand, by reducing the possibility of movement of the amino terminal part with respect to the catechol portion, the molecule's entry into the catalytic site is completely prevented and molecules (**4** and **5**) were inactive. Our results confirmed that a certain degree of chain flexibility is necessary in order to facilitate the interaction of the ligands with the catalytic site.

Despite our chemical modifications, a clear understanding of the optimal length and flexibility of the tail portion of the ligand would come only from the successful determination of the crystal structure of a PDE4D-ligand complex that includes also the portion of the regulatory domain that caps the entrance of the catalytic pocket of the enzyme. Such structure would provide the necessary evidence of the interactions that are needed to stabilize the protein ligand complex and, possibly, to favor selectivity over different PDE4 isoforms. Further studies aimed at obtaining new inhibitors that can interact more efficiently both with the catalytic and with the regulatory domains of long PDE4D isoforms are ongoing.

4. Materials and Methods

4.1. Chemistry

All chemicals were obtained from Sigma-Aldrich s.r.l. (Milan, Italy). All compounds were tested for purity by TLC (Kieselgel 60F254 DC-Alufolien, E. Merck, Darmstadt, Germany). Product purification, when necessary, was performed by using Flash Isolera One Biotage instrument, Silicagel column SNAP ULTRA-HP SpherETM 25 μm.

Melting points are not corrected and were measured with a Buchi 540 instrument.

IR spectra were recorded with a Perkin-Elmer 390 spectrophotometer or a Spectrum Two FT-IR Spectrometer (PerkinElmer, Inc., Waltham, MA, USA).

^{1}H NMR spectra were recorded on a Varian Gemini 200 (200 MHz) instrument or BRUKER DPX-300 (300 MHz); chemical shifts were referred to as δ (ppm) relative to tetramethylsilane (TMS) as internal standard; signals were characterized as s (singlet), d (doublet), t (triplet), q (quartet), sept (septet), m (multiplet), or br s (broad signal); *J* were reported in Hertz. ^{13}C NMR spectra were recorded on a BRUKER DPX-300 (300 MHz) or a JEOL JNM ECZ-400S/L1 (400 MHz).

Elemental analyses were within 0.4% of the theoretical values and were determined with an EA 1110 elemental analyzer (Fison-Instruments, Milan, Italy). Table of elemental analyses data and images of all IR, 1H NMR an 13C NMR are available in online Supplementary materials.

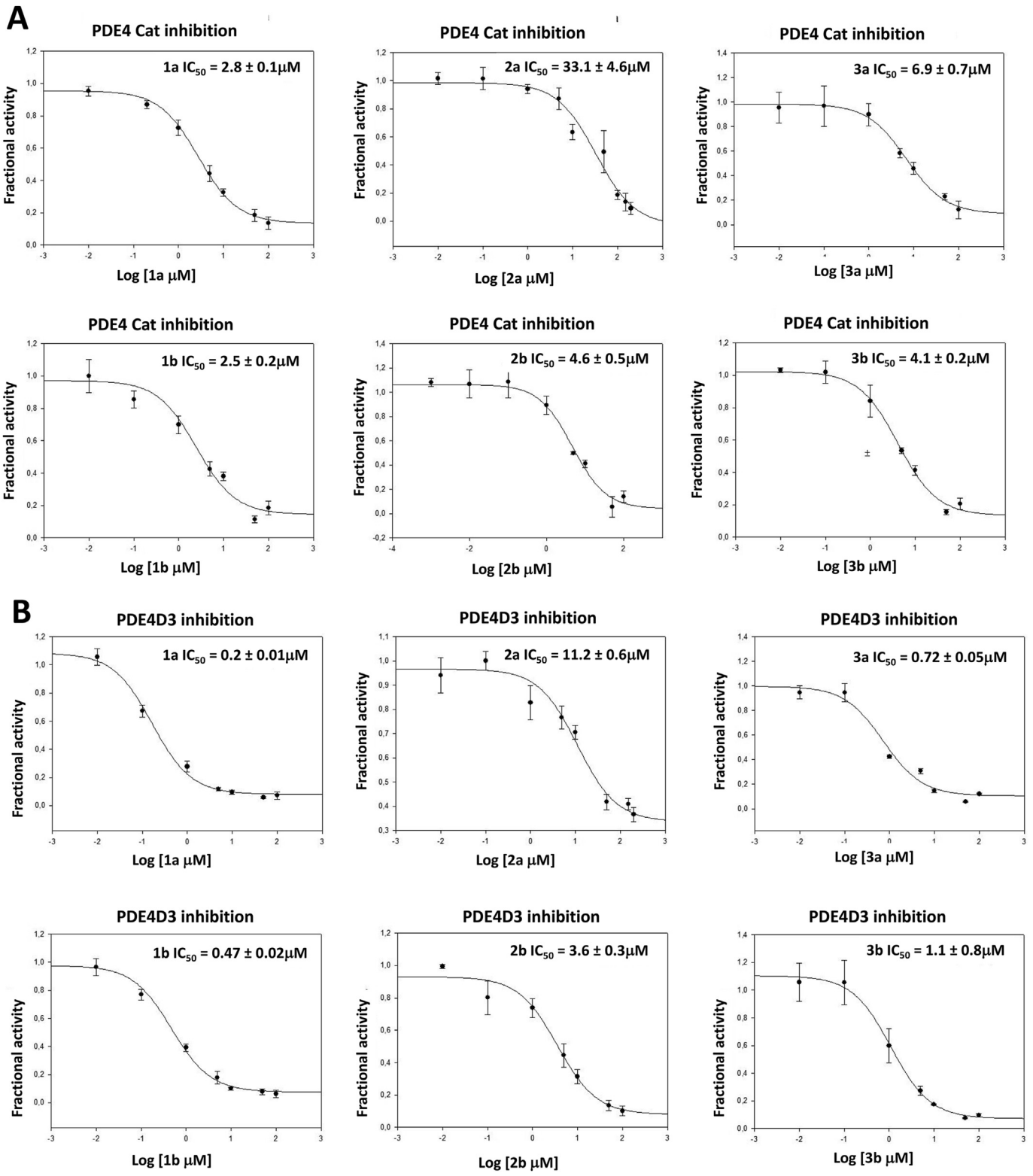

Fig. 5. IC_{50} curves for the most active compounds (**1a**, **1b**, **2a**, **2b**, **3a**, **3b**) relative to the catalytic domain only (A) and against the long PDE4D3 isoform (B). The experimental conditions are reported in the Materials and Methods section. The reported data are the mean values of three replicates ± SD (standard deviation).

4.1.1. Synthesis of 1-[3-(cyclopentyloxy)-4-methoxyphenyl]ethanol ***7***

To a mixture of magnesium turniture (0.67 g, 28 mmol) and I_2 (trace) in an. diethyl ether (10 mL) CH_3I (3.8 g, 1.67 mL, 28 mmol) solved in an. diethyl ether (10 mL) was slowly added and the temperature was maintained at 30 °C until magnesium disappears. The reaction mixture was cooled with an ice bath and the 3-(cyclopentyloxy)-4-methoxybenzaldehyde **6** (5.0 g, 22 mmol) solved in an. diethyl ether (10 mL) was slowly added and the mixture was stirred at 30–40 °C for 3 hs. Then, ice water and

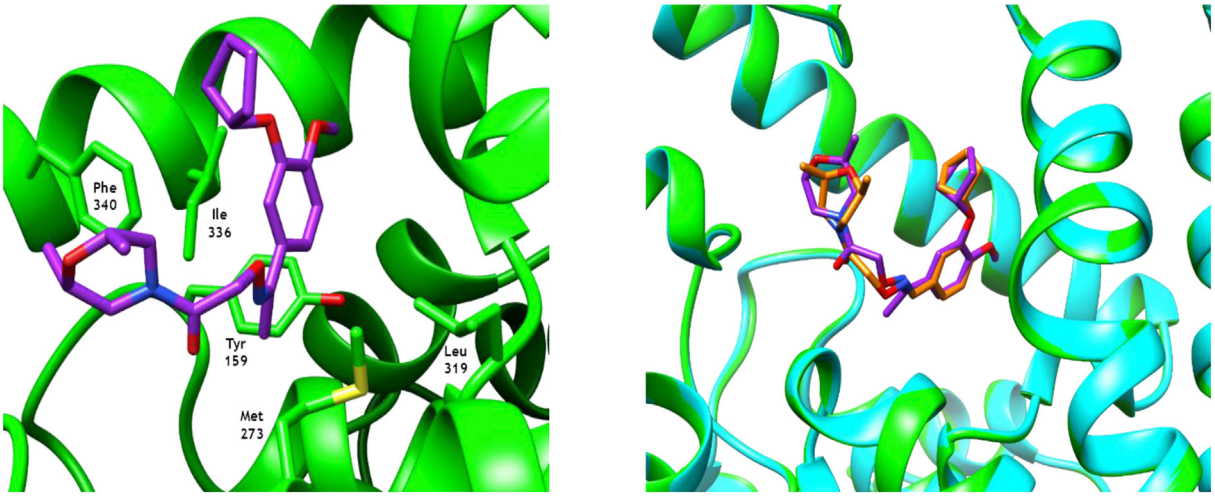

Fig. 6. A) Crystal structure of the PDE4D catalytic domain in complex with **1b** (GEBR-41b) (PDB code: 7AY6), featuring the ligand in a protruding conformation. The side chains of hydrophobic amino acids that make contacts with the methyl group in the linker region are shown as sticks. **B)** Structure superposition of the GEBR-41b complex (ligand shown in purple) with the PDE4D catalytic domain in complex with GEBR-7b (ligand shown in orange) (PDB code: 6F6U). The two ligands, which differ only for the methyl group in the linker region, are almost completely superimposable (rmsd 0.649 Å). Here, the side chains of the amino acids contacting the methyl group of GEBR-41b are omitted for clarity. The 2Fo-Fc electron density map of the ligand is shown in the Supp. Inf. (Fig. S1). Figures were created using Pymol [29].

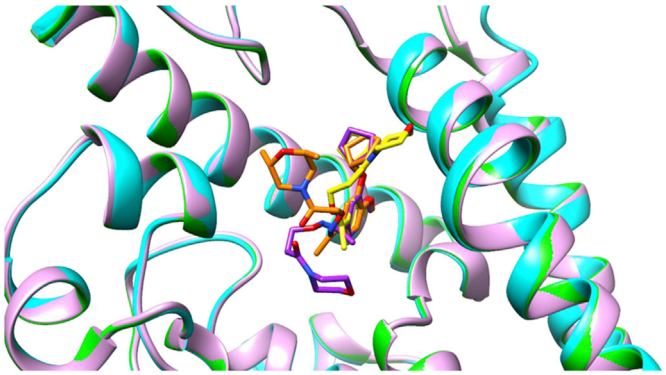

Fig. 7. Structure superposition of the two monomers of the PDE4D catalytic domain in complex with **2a** (GEBR-42a) (PDB code: 7B9H) and with **1b** (GEBR-41b) (PDB code: 7AY6). The ligands in the **2a** complex structure bind in two different conformations: while in one monomer it adopts a protruding conformation (shown in yellow), in the other (shown in purple) it is twisted toward the bottom of the catalytic pocket and features van der Waals contacts between the morpholine moiety and the methyl group in the linker region. As a comparison, the protein structure of the **1b** complex is depicted in light violet and the **1b** compound in orange. The 2Fo-Fc electron density map of the ligands are shown in the Supp. Inf. (Fig. S1).

saturated NH_4Cl solution (15 mL) was added and the aqueous phases were extracted with diethyl ether (2 × 20 mL). The combined organic phases were washed with brine (50 mL), dried (Na_2SO_4) and concentrated under reduced pressure to obtain a yellow oil, which crystallizes as white solid from diethyl ether. Yield: 100%.

4.1.2. Synthesis of 1-[3-(cyclopentyloxy)-4-methoxyphenyl] ethanone ***8***

To a suspension of pyridinium chlorochromate (3.2 g, 15 mmol) in cycloexane (5 mL) a solution of **7** (2.36 g, 10 mmol) solved in cycloexane (10 mL) is added and the mixture was heated at 70 °C for 3 hs. After cooling to room temperature, diethyl ether was repeatedly added (5 × 10 mL), the gummy black residue was washed, and the organic yellow solution decanted. The combined organic phases were then washed with 1 M NaOH (15 mL), brine (15 mL), dried (Na_2SO_4) and concentrated under reduced pressure to obtain a yellow oil which crystallized as white solid from diethyl ether. Mp: 127–129 °C Yield: 94% (lett 95%) [21].

4.1.3. Synthesis of (1Z)-1-[3-(cyclopentyloxy)-4-methoxyphenyl] ethanone oxime ***9***

To a solution of ketone **8** (1.1 g, 4.69 mmol) in 96% EtOH (10 mL) hydroxylamine hydrochloride (0.7 g, 10 mmol) solved in water (10 mL), $NaHCO_3$ (0.84 g, 10 mmol) and water (10 mL) were added and the mixture was stirred at 60 °C for 4 hs. After cooling to room temperature, the reaction mixture was poured into ice water (50 mL) to obtain a solid which was filtered, washed with water and recrystallized from 95% EtOH to obtain a yellowish solid. Yield: 63%. Mp: 95–97 °C [22]. IR (KBr) cm^{-1}: 3254 (OH). ^1H NMR (300 MHz, $CDCl_3$): δ 1.50–2.10 (m, 8H, cyclopent.), 2.27 (s, 3H, CH_3), 3.90 (s, 3H, OCH_3), 4.78–4.95 (m, 1H, OCH cyclopent.), 6.15 (brs, 1H, OH disappears with D_2O), 6.88 (d, J = 8.0 Hz, 1H, H-5 Ar), 7.14 (dd, J = 8.0 Hz, 2.0 Hz, 1H, H-6 Ar), 7.28 (d, J = 2.0 Hz, 1H, H-2 Ar). ^{13}C NMR (101 MHz, $CDCl_3$) δ 155.55, 147.03, 129.07, 119.00, 112.03, 111.07, 80.05, 77.23, 76.88, 76.06, 56.00, 32.88, 24.22, 12.03. Anal. Calcd. for $C_{14}H_{19}NO_3$.

4.1.4. General procedure for the synthesis of derivatives ***1a*** and ***1b***

Into a solution of **9** (0.249 g, 1 mmol) in anhydrous DMF (2 mL) K_2CO_3 (0.414 g, 3 mmol) was suspended; then, 4-(chloroacetyl)morpholine or 4-(chloroacetyl)2,6-dimethylmorpholine (3 mmol) solved in anhydrous DMF (2 mL) was added dropwise and the mixture was heated at 50–60 °C for 18 hs under nitrogen atmosphere. After cooling to room temperature, the mixture is poured into water (100 mL) and extracted with AcOEt (2 × 20 mL); the organic phases are washed with brine (3 × 20 mL), water (3 × 20 mL), dried ($MgSO_4$) and concentrated under reduced pressure to obtain yellowish oils which were purified by flash chromatography, using diethyl ether as eluent.

4.1.4.1. (1Z)-1-[3-(cyclopentyloxy)-4-methoxyphenyl]ethanone O-(2-morpholin-4-yl-2oxoethyl) oxime ***1a***. Yellow oil. Yield: 57%. IR ($CHCl_3$): cm^{-1} 1673 (CO). ^1H NMR ($CDCl_3$): δ 1.56–2.03 (m, 8H, $4CH_2$ cyclopent.), 2.29 (s, 3H, CH_3), 3.38–3.80 (m, 8H, $4CH_2$ morph.), 3.89 (s, 3H, OCH_3), 4.63–4.81 (m, 1H, OCH cyclopent.), 4.87 (s, 2H,

Table 3
Data collection and refinement statistics[a].

	GEBR-41-b	GEBR-42-a
Wavelength (Å)	1.00	1.00
Resolution range (Å)	64.84–1.66 (1.69–1.66)	54.13–1.50 (1.53–1.50)
Space group	P 2_1 2_1 2_1	P 2_1 2_1 2_1
Unit cell (a, b, c) (Å)	64.84, 98.66, 120.24	64.75, 98.63, 119.82
Total reflections	174845 (15148)	245551 (23667)
Unique reflections	89739 (8130)	122897 (11934)
Multiplicity	5.70 (5.50)	12.90 (10.10)
Completeness (%)	98.50 (90.10)	99.80 (97.70)
Mean I/σ(I)	9.10 (1.20)	11.50 (1.40)
Wilson B-factor (Å^2)	17.33	18.44
R-merge	0.108 (1.31)	0.115 (2.023)
CC1/2	0.996 (0.600)	0.999 (0.631)
Reflections used in refinement	89592 (8076)	122638 (11909)
Reflections used for R-free	4517 (432)	6199 (632)
R-work	0.1828 (0.2653)	0.1938 (0.3668)
R-free	0.2153 (0.3038)	0.2201 (0.3806)
Number of non-hydrogen atoms	6264	6331
Protein	5411	5460
Ligands	124	182
Solvent	729	689
Protein residues	659	659
RMS(bonds) (Å)	0.014	0.009
RMS(angles) (°)	1.44	1.11
Ramachandran favored (%)	98.02	97.86
Ramachandran allowed (%)	1.83	1.68
Ramachandran outliers (%)	0.15	0.46
Rotamer outliers (%)	0.32	0.80
Clashscore	4.91	5.51
Average B-factor (Å^2)	25.69	27.94
Protein	24.14	26.52
Ligands	37.65	37.57
Solvent	35.19	36.61

[a] Statistics for the highest-resolution shell are shown in parentheses.

CH_2CO), 6.87 (d, J = 8.0 Hz, 1H, H-5 Ar) 7.17 (dd, J = 8.0, 2.0 Hz, 1H, H-6 Ar) 7.27 (d, J = 2.0 Hz, 1H, H-2 Ar). ^{13}C (101 MHz $CDCl_3$): δ 167.60, 156.21, 151.52, 147.78, 128.55, 119.42, 113.47, 112.69, 111.24, 80.67, 72.71, 66.98, 66.59, 56.09, 45.79, 42.32, 32.83, 24.14, 12.95. Anal. ($C_{20}H_{28}N_2O_5$) C, H, N.

4.1.4.2. (1Z)-1-[3-(cyclopentyloxy)-4-methoxyphenyl]ethanone O-[2-(2,6-dimethylmorpholin-4-yl)-2oxoethyl] oxime ***1b***. Yellow oil. Yield: 87%. IR ($CHCl_3$): cm^{-1} 1671 (CO). ^{1}H NMR ($CDCl_3$): δ 1.13–1.37 (m, 6H, $2CH_3$), 1.55–2.02 (m, 8H, $4CH_2$ cyclopent.), 2.27 (s, 3H, CH_3), 2.33–2.48 and 2.76–2.87 (2 m, 2H, 2CHO morph.), 3.40–3.72 (m, 4H, $2CH_2N$ morph.), 3.88 (s, 3H, OCH_3), 4.32–4.64 (m, 1H, OCH cyclopent.), 4.86 (s, 2H, CH_2CO), 6.85 (d, J = 8.0 Hz, 1H, H-5 Ar) 7.18 (dd, J = 8.0, 2.0 Hz, 1H, H-6 Ar) 7.29 (d, J = 2.0 Hz, 1H, H-2 Ar). ^{13}C NMR (101 MHz, $CDCl_3$): δ 167.28, 156.21, 151.57, 147.55, 128.50, 119.45, 113.52, 112.75, 111.25, 80.69, 72.85, 72.04, 71.79, 56.17, 51.89, 50.87, 47.37, 40.87, 32.89, 24.19, 18.83, 12.92. Anal. ($C_{22}H_{32}N_2O_5$) C, H, N.

4.1.5. Synthesis of (1Z)-1-[3-(cyclopentyloxy)-4-methoxyphenyl] ethanone O-[2-(4-hydroxypiperidin-1-yl)-2oxoethyl] oxime ***1c***

Sodium ethoxide was prepared from Na (35 mg, 1.5 mmol) and absolute EtOH (10 mL). The solvent was evaporated under reduced pressure and compound **9** (0.373 g, 1.5 mmol) solved in an. DMF (10 mL) was added to the white solid residue. After stirring for 20 min, 1-(chloroacetyl)piperidin-4-ol (0.532 mg, 3 mmol) solved in an. DMF (1 mL) was added dropwise and the mixture was stirred at 50–60 °C for 24 hs under nitrogen atmosphere. After cooling to room temperature, the mixture was poured into water (50 mL) and extracted with AcOEt (2 × 20 mL); the organic phases were washed with brine (3 × 20 mL), water (3 × 20 mL), dried ($MgSO_4$) and concentrated under reduced pressure to obtain a yellow oil which was purified by flash chromatography, using as the eluent firstly dietyl ether, then a mixture of diethyl ether/methanol (8:2) Yellow oil. Yield: 42%. IR ($CHCl_3$) cm^{-1}: 2949 (OH), 1644 (CO). ^{1}H NMR ($CDCl_3$): δ 1.32–1.94 (m, 12H, $4CH_2$ cyclopent. + $2CH_2$pip.), 2.20 (s, 3H, CH_3), 3.04–3.23 (m, 2H, CH_2N pip.), 3.40–3.55 (m, 2H, CH_2N pip.), 3.78 (s, 3H, OCH_3), 3.82–4.01 (m, 1H, CHOH pip.), 4.70–4.84 (m, 3H, OCH cyclopent. + CH_2CO), 6.77 (d, J = 8.6 Hz, 1H, H-5 Ar) 7.06 (dd, J = 8.6, 2.0 Hz, 1H, H-6 Ar) 7.18 (d, J = 2.0 Hz, 1H, H-2 Ar). ^{13}C (CDCl3): δ 168.19, 155.35, 151.53, 147.23, 128.89, 121.39, 113.24, 111.52, 81.10, 70.61, 67.25, 56.09, 43.24, 34.03, 32.81, 23.45, 16.76. Anal. ($C_{21}H_{30}N_2O_5$) C, H, N.

4.1.6. General procedure for the synthesis of derivatives ***2a*** *and* ***2b***

To a solution of oxime **9** (0.373 g, 1.5 mmol) in an. DMF (2 mL), NaH (in a 50% mineral dispersion, 0.15 g, 3 mmol) was added at 0 °C and the mixture was stirred at room temperature for 2 hs. Then, 4-(3-chloropropanoyl)morpholine or 4-(3-chloropropanoyl)-2,6-dimethylmorpholine (3 mmol) solved in an. DMF (2 mL) was slowly added at 0 °C and the reaction mixture was stirred at room temperature for 18 h under nitrogen atmosphere. The mixture was poured into water (50 mL) and extracted with diethyl ether (2 × 20 mL); the organic phases were washed with brine (3 × 20 mL), water (3 × 20 mL), dried ($MgSO_4$) and evaporated under reduced pressure to obtain a yellow oil which was purified by flash chromatography, using diethyl ether as eluent.

4.1.6.1. (1Z)-1-[3-(cyclopentyloxy)-4-methoxyphenyl]ethanone O-(3-morpholin-4-yl-3-oxopropyl) oxime ***2a***. Yellow oil. Yield: 56%. IR (film): cm-^{1}1630 (CO). ^{1}H NMR ($CDCl_3$): δ 1.53–2.04 (m, 8H, $4CH_2$ cyclopent.), 2.21 (s, 3H, CH_3), 2.81 (t, J = 7.0 Hz, 2H, CH_2CO), 3.48–3.59 (m, 4H, $2CH_2N$ morph.), 3.62–3.74 (m, 4H, $2CH_2O$ morph.), 3.87 (s, 3H, OCH_3), 4.50 (t, J = 7.0 Hz, 2H, CH_2O), 4.78–4.83

(m, 1H, OCH cyclopent.), 6.88 (d, J = 10.0 Hz, 1H, H-5 Ar) 7.17 (dd, J = 10.0, 2.0 Hz, 1H, H-6 Ar) 7.29 (d, J = 2.0 Hz, 1H, H-2 Ar). ^{13}C (101 MHz, $CDCl_3$): δ 170.26, 155.88, 151.74, 147.64, 128.32, 119.56, 112.64, 111.28, 80.73, 70.45, 66.81, 56.12, 32.88, 32.84, 24.21, 24.09, 13.02. Anal. ($C_{21}H_{30}N_2O_5$) C, H, N.

4.1.6.2. (1Z)-1-[3-(cyclopentyloxy)-4-methoxyphenyl]ethanone O-[3-(2,6-dimethylmorpholin-4-yl)-3-oxopropyl] oxime ***2b***. Yellow oil. Yield: 24%. IR (film): cm^{-1} 1640 (CO). ^{1}H NMR ($CDCl_3$): δ 1.09–1.32 (m, 6H, $2CH_3$ morph.), 1.55–2.02 (m, 8H, $4CH_2$ cyclopent.), 2.20 (s, 3H, CH_3), 2.64–2.90 (m, 6H, $2CH_2N$ morph. + CH_2CO), 3.39–3.64 (m, 2H, 2CHO morph.), 3.87 (s, 3H, OCH_3), 4.38–4.58 (m, 2H, CH_2O) 4.73–4.83 (m, 1H, OCH cyclopent.), 6.84 (dd, J = 10.0 Hz, 1H, H-5 Ar) 7.11 (dd, J = 10.0, 1.8 Hz, 1H, H-6 Ar) 7.28 (dd, J = 1.8 Hz, 1H, H-2 Ar). ^{13}C (101 MHz $CDCl_3$): δ 169.72, 154.88, 151.38, 147.55, 129.01, 128.44, 127.43, 119.18, 112.57, 111.28, 80.68, 71.95, 70.36, 56.38, 33.23, 32.91, 24.08, 18.82, 12.78. Anal. ($C_{23}H_{34}N_2O_5$) C, H, N.

4.1.7. Synthesis of 1-[3-(cyclopenthyloxy)-4-methoxyphenyl] ethanone O-(oxiran-2-ylmethyl)-oxime ***10***

To a sodium ethoxide solution prepared from sodium (0.27 g, 11.3 mmol) and absolute ethanol (20 mL) a solution of oxime **9** (2.82 g, 11.32 mmol) in absolute EtOH (10 mL) was added and the mixture was stirred at room temperature for 20 min. The solvent was evaporated under reduced pressure and the residue was suspended in anhydrous DMF (20 mL); then, epichlorohydrin (1.6 mL, 17 mmol) solved in anhydrous DMF (2 mL) was slowly added and the mixture was heated at 40–50 °C for 12 hs. After cooling to room temperature, the mixture was poured into water (50 mL) and extracted with diethyl ether (3 × 20 mL); the organic phases were washed with water (3 × 20 mL), brine (20 mL), dried ($MgSO_4$) and evaporated under reduced pressure to obtain a yellow oil which was purified by flash chromatography using DCM as eluent. Yellow oil. Yield: 53%. IR (KBr): cm^{-1} 1672 (C=N). ^{1}H NMR ($CDCl_3$): δ 1.51–2.05 (m, 8H, cyclopent.), 2.25 (s, 3H, CH_3), 2.65–2.96 (m, 2H, CH_2O epox.), 3.16–3.45 (m, 1H, CHO epox.), 3.86 (s, 3H OCH_3), 4.00–4.45 (m, 2H, OCH_2), 4.75–4.90 (m, 1H, OCH cyclopent.), 6.84 (d, J = 8.0 Hz, 1H, H-5 Ar), 7.15 (dd, J = 8.0 Hz, 2.0 Hz, 1H, H −6 Ar), 7.28 (d, J = 2.0 Hz, 1H, H-2 Ar). Anal. ($C_{17}H_{23}NO_4$) C,H,N.

4.1.8. General procedure for the synthesis of derivatives ***3a*** *and* ***3b***

To oxirane **10** (0.60 g, 1.96 mmol) morpholine or 2,6-dimethylmorpholine (4 mL) was added and the mixture was heated at 60 °C for 18 h. After cooling to room temperature, the mixture was poured into water (50 mL) and the aqueous phase was extracted with dietyl ether (3 × 20 mL); then, the organic phases were washed with water (2 × 20 mL), dried ($MgSO_4$) and concentrated under reduced pressure to obtain yellow oils which were purified by flash chromatography using as the eluents, firstly dietyl ether, then a mixture of dietyl ether/methanol (9:1).

4.1.8.1. (1Z)-1-[3-(cyclopentyloxy)-4-methoxyphenyl]ethanone O-(2-hydroxy-3-morpholin-4-ylpropyl) oxime ***3a***. Yellow oil. Yield: 88%. IR ($CHCl_3$): cm^{-1} 3452 (OH). ^{1}H NMR ($CDCl_3$): δ 1.52–2.02 (m, 8H, 4 CH_2 cyclopent.), 2.24 (s, 3H, CH_3), 2.41–2.75 (m, 6H, $3CH_2N$), 3.66–3.80 (m, 4H, $2CH_2O$ morph.), 3.86 (s, 3H, OCH_3), 4.05–4.30 (m, 3H, OCH_2 + CH–OH), 4.75–4.90 (m, 1H, OCH cyclopent.), 6.85 (d, J = 10.0 Hz, 1H, H-5 Ar), 7.14 (dd, J = 10.0, 2.0 Hz, 1H, H-6 Ar), 7.25 (d, J = 2.0 Hz, 1H, H-2 Ar). ^{13}C (101 MHz $CDCl_3$): δ 155.02, 151.30, 147.51, 128.99, 119.13, 112.56, 111.32, 80.61, 77.51, 67.00, 66.56, 65.83, 61.29, 56.02, 53.89, 32.75, 24.10, 15.26, 12.69. Anal. ($C_{21}H_{32}N_2O_5$) C, H, N.

4.1.8.2. (1Z)-1-[3-(cyclopentyloxy)-4-methoxyphenyl]ethanone O-[3-(2,6-dimethylmorpholin-4-yl)-3-hydroxypropyl] oxime ***3b***. Yellow oil. Yield: 96%. IR ($CHCl_3$): cm^{-1} 3445 (OH). ^{1}H NMR ($CDCl_3$): δ 1.10–1.30 (m, 6H, $2CH_3$ morph.), 1.51–2.08 (m, 8H, cyclopent.), 2.25 (s, 3H, CH_3), 2.35–2.94 (m, 6H, $3CH_2N$), 3.62–3.85 (m, 2H, $2CH_2O$ morph.), 3.88 (s, 3H, OCH_3), 4.10–4.30 (m, 3H, OCH_2 + CH–OH), 4.79–4.90 (m, 1H, OCH cyclopent.), 6.86 (d, J = 8.0 Hz, 1H, H-5 Ar), 7.16 (dd, J = 8.0, 2.0 Hz, 1H, H-6 Ar), 7.28 (d, J = 2.0 Hz, 1H, H-2 Ar). ^{13}C NMR (101 MHz, $CDCl_3$) δ 155.37, 151.40, 147.56, 128.88, 119.21, 112.48, 111.28, 80.62, 75.98, 66.18, 61.26, 60.14, 58.21, 56.19, 32.91, 24.21, 18.97, 12.82. Anal. ($C_{23}H_{36}N_2O_5$) C, H, N.

4.1.9. Synthesis of (1Z)-1-[3-(cyclopentyloxy)-4-methoxyphenyl] ethanone O-[2-hydroxy-3-(4-hydroxypiperidin-1-yl)propyl] oxime ***3c***

To a solution of oxirane **10** (1.26 g, 4.13 mmol) in an. DMF (10 mL) piperidin-1-ol (0.83 g, 8.26 mmol) solved in an. DMF (2 mL) was added and the reaction mixture was stirred at 60 °C for 18 hs. After cooling to room temperature, the reaction mixture was poured into water (50 mL); the aqueous phase was extracted with dietyl ether (3 × 20 mL); the organic phase was washed with water (2 × 20 mL), brine (3 × 20 mL), dried ($MgSO_4$) and concentrated under reduced pressure to obtain a yellow oil which was purified by flash chromatography using as eluents firstly dietyl ether, then a mixture of dietyl ether/methanol (9:1). Finally, the crude oil was crystallized by adding petroleum ether (p.eb. 40–60 °C). White solid. Mp: 51–52 °C. Yield: 34%. IR ($CHCl_3$): cm^{-1} 3429 (OH). ^{1}H NMR ($CDCl_3$): δ 1.50–2.06 (m, 12H, $4CH_2$ cyclopent. + $2CH_2$ pip.), 2.24 (s, 3H, CH_3), 2.47–2.65 (m, 2H, CH_2N), 2.75–3.08 (m, 4H, $2CH_2N$ pip.), 3.70–3.79 (m, 1H, OCH pip.), 3.87 (s, 3H, OCH_3), 4.10–4.30 (m, 3H, OCH_2 + CH–OH), 4.75–4.90 (m, 1H, OCH cyclopent.), 6.87 (d, J = 8.0 Hz, 1H, H-5 Ar), 7.15 (dd, J = 8.0, 2.0 Hz, 1H, H-6 Ar), 7.25 (d, J = 2.0 Hz, 1H, H-2 Ar). ^{13}C (101 MHz, $CDCl_3$): δ 155.38, 151.53, 147.23, 128.75, 121.39, 113.26, 111.52, 81.10, 75.39, 67.09, 66.42, 60.80, 56.09, 51.30, 34.69, 32.81, 23.45, 16.78. Anal. ($C_{22}H_{34}N_2O_5$) C, H, N.

4.1.10. Synthesis of 3-(4-hyidroxy-3-methoxyphenyl)propionic acid ***12***

A solution of *trans*-ferulic acid **11** (0.3 g, 1.54 mmol) in MeOH (14 mL) was reduced with H-CUBE apparatus at room temperature in full H_2 mode (flow = 1 mL/min) using 5% Pd/C as catalyst. The obtained solution was concentrated under reduced pressure to afford the product as white solid. Mp: 88.5–90.0 °C Yield:100% (lit.: Mp 91–92 °C, Yield 98%) [26].

4.1.11. Synthesis of 6-hydroxy-5-methoxyindan-1-one ***13***

A solution of **12** (1.2 g, 6.12 mmol) in methanesulfonic acid (5 mL) was heated to 90 °C under nitrogen atmosphere and the reaction was stirred and monitored by TLC until acid **12** disappears. After cooling to room temperature, the reaction mixture was carefully poured into water (100 mL); the aqueous phase is extracted with DCM (3 × 30 mL), the organic phases were washed with water (3 × 20 mL), dried ($MgSO_4$) and concentrated under reduced pressure to obtain a dark solid. Mp: 189–190 °C [lit: 194 °C] Yield: 56% (lit: 65% [30].

4.1.12. Synthesis of 6-cyclopentyloxy-5-methoxyindan-1-one ***14***

To a solution of indanone **13** (0.356 g, 2 mmol) in an. DMF (10 mL) K_2CO_3 (0.41 g, 3 mmol) and KI (0.01 g, 0.06 mmol) were added and the suspension was heated at 65 °C. Then cyclopentyl bromide (0.38 g, 2.57 mmol) was slowly added and the mixture was stirred at 65 °C for 22 hs. After cooling to room temperature, toluene (50 mL) was added; the organic phase was washed with 1 M NaOH (2 × 20 mL) and the combined aqueous phases were extracted with toluene (20 mL); the organic phases were washed

with H_2O (3 × 20 mL), dried ($MgSO_4$) and concentrated under reduced pressure to obtain a yellow oil which was then used without further purification. Yield: 73%. IR ($CHCl_3$): cm^{-1} 1694 (CO). ^1H NMR ($CDCl_3$): δ 1.512.11 (m, 8H, $4CH_2$ cyclopent.), 2.67 (t, J = 5.0 Hz, 2H, CH_2), 3.01 (t, J = 5.0, 2H, CH_2), 3.93 (s, 3H OCH_3), 4.72–4.86 (m, 1H, OCH cyclopent.), 6.87 (s, 1H, Ar), 7.17 (s, 1H, Ar). Anal. calcd. for ($C_{15}H_{18}O_3$):

*4.1.13. Synthesis of (1E)-6-(cyclopentyloxy)-5-methoxyindan-1-one oxime **15***

To a solution of indanone **14** (0.40 g, 1.62 mmol) in 95% ethanol (4.5 mL) hydroxylamine hydrochloride (0.5 g, 6.48 mmol) solved in water (2 mL) was added. Then, $NaHCO_3$ (0.55 g, 6.48 mmol) and water (3 mL) were added to small portions and the reaction mixture was heated at 60 °C for 2 hs. After cooling to room temperature, the mixture was poured into water (50 mL). The solid obtained was filtered, washed with water and recrystallized from 95% ethanol. Ivory solid. Mp: 138–140 °C. Yield: 59%. IR (KBr): cm^{-1} 1689 (C=N), 1049 (N–O). ^1H NMR ($CDCl_3$): δ 1.50–2.13 (m, 8H, $4CH_2$ cyclopent.), 2.60–2.90 (m, 2H, CH_2), 3.60–3.72 (m, 2H, CH_2), 3.84 (s, 3H OCH_3), 4.69–4.89 (m, 1H, CHO cyclopent.), 6.74 (s, 1H, Ar), 6.80 (s, 1H, Ar). ^{13}C NMR ($CDCl_3$, 300 MHz): δ 24.15, 26.61, 28.35, 32.75, 56.05, 80.40, 106.49, 107.81, 127.96, 141.53, 147.60, 152.77, 164.36. Anal. Calcd. for ($C_{15}H_{19}NO_3$).

*4.1.14. General procedure for the synthesis of derivatives **4a–c***

To a solution of **15** (0.261 g, 1 mmol) in anhydrous DMF (2 mL) K_2CO_3 (0.414 g, 3 mmol) and 4-(chloroacetyl)morpholine or 4-(chloroacetyl)2,6-dimethylmorpholine or 1-(chloroacetyl)piperidin-4-ol (3 mmol) solved in anhydrous DMF (2 mL) were added dropwise and the mixture was heated at 50–60 °C for 18 hs under nitrogen atmosphere. After cooling to room temperature, the mixture was poured into water (100 mL) and extracted with AcOEt (2 × 20 mL); the organic phases were washed with brine (3 × 20 mL), water (3 × 20 mL), dried ($MgSO_4$) and concentrated under reduced pressure to obtain yellow oils which were purified by flash chromatography, using diethyl ether as eluent.

*4.1.14.1. (1E)-6-(cyclopentyloxy)-5-methoxyindan-1-one O-(2-morpholin-4-yl-2-oxoethyl)oxime **4a**.* Ivory solid. Mp: Yield: 44%. IR ($CHCl_3$): cm^{-1} 1643 (CO), 1603 (C=N). ^1H NMR ($CDCl_3$): δ 1.53–2.13 (m, 8H, $4CH_2$ cyclopent.), 2.95–3.12 (m, 4H, $2CH_2$), 3.57–3.83 (m, 8H, $4CH_2$ morph.), 3.89 (s, 3H, OCH_3), 4.78–4.95 (m, 3H, OCH cyclopent. + CH_2CO), 6.80 (s, 1H, Ar), 7.17 (s, 1H, Ar). ^{13}C (101 MHz, $CDCl_3$): δ 167.76, 164.64, 153.19, 147.63, 141.87, 127.58, 107.82, 106.81, 80.57, 77.24, 77.19, 77.12, 72.72, 66.86, 56.07, 45.78, 42.29, 32.75, 28.41, 27.28, 24.07 Anal calcd ($C_{21}H_{28}N_2O_5$) C, H, N.

*4.1.14.2. (1E)-6-(cyclopentyloxy)-5-methoxyindan-1-one O-[2-(2,6-dimethylmorpholin-4-yl)-2-oxoethyl]oxime **4b**.* Yellow oil. Yield: 46%. IR ($CHCl_3$): cm^{-1} 1641 (CO), 1603 (C=N). ^1H NMR ($CDCl_3$): δ 1.22 (d, J = 6.2, 6H, $2CH_3$), 1.51–2.03 (m, 8H, $4CH_2$ cyclopent.), 2.86–3.08 (m, 4H, $2CH_2$), 3.40–3.78 (m, 4 H, $2CH_2N$ morph.), 3.88 (s, 3H, OCH_3), 3.90–4.15 (m, 1H, CHO morph.), 4.38–4.55 (m, 1H, CHO morph.), 4.76–4.96 (m, 3H, OCH cyclopent. + CH_2CO), 6.74 (s, 1H, Ar), 7.13 (s, 1H, Ar). ^{13}C (101 MHz, CDCl3): δ 169.44, 163.27, 152.17, 144.54, 139.66, 131.87, 109.34, 107.69, 81.11, 70.73, 69.56, 56.02, 52.44, 32.81, 27.99, 25.09, 23.45, 18.03. Anal calcd ($C_{23}H_{32}N_2O_5$) C, H, N.

*4.1.14.3. (1E)-6-(cyclopentyloxy)-5-methoxyindan-1-one O-[2-(4-hydroxypiperidin-1-yl)-2-oxoethyl]oxime **4c**.* Yellow oil. Yield: 41%. IR ($CHCl_3$): cm^{-1} 1638 (CO), 1604 (C=N). ^1H NMR ($CDCl_3$): δ 1.50–2.12 (m, 8H, $4CH_2$ cyclopent.), 2.81–3.02 (m, 4H, $2CH_2$), 3.15–3.38 (m, 4H, $2CH_2$ pip.), 3.63–3.74 (m, 2H, CH_2N pip), 3.89 (s, 3H, OCH_3), 4.00–4.18 (m, 2H, CH_2N pip.), 4.68–4.95 (m, 4H, CH_2CO + OCH cyclopent. + CHOH pip.), 6.80 (s, 1H, Ar), 7.30 (s, 1H, Ar). ^{13}C (101 MHz, $CDCl_3$): δ 169.39, 163.27, 152.17, 144.54, 139.66, 131.87, 109.34, 107.69, 81.11, 70.53, 67.25, 56.02, 43.24, 34.03, 32.81, 27.99, 25.09, 23.45. Anal calcd ($C_{22}H_{30}N_2O_5$) C, H, N.

*4.1.15. Synthesis of (1E)-6-(cyclopentyloxy)-5-methoxyidan-1-one-O-(oxiran-2ylmethyl) oxime **16***

To a sodium ethoxide solution prepared from Na (0.14 g, 5 mmol) in absolute EtOH (9.34 mL) a solution of oxime **15** (1.31 g, 5 mmol) in absolute EtOH (10 mL) was added and the mixture was stirred at room temperature for 20 min. Then, the solvent was evaporated under reduced pressure, the obtained crude was solved in an. DMF (10 mL) and epichlorohydrin (0.93 g, 10 mmol) was added dropwise. The mixture was heated at 40–50 °C for 18 hs. After cooling to room temperature, the reaction mixture is poured into water (50 mL) and the aqueous solution is extracted with diethyl ether (3 × 20 mL); the organic phase was washed with water (3 × 20 mL), brine (20 mL), dried ($MgSO_4$) and concentrated under reduced pressure to obtain a yellow oil which was purified by flash chromatography on silica gel using diethyl ether as eluent. Yield: 50%. ^1H NMR ($CDCl_3$): δ 1.51–2.10 (m, 8H, $4CH_2$ cyclopent.), 2.60–2.80 and 2.84–3.06 (2 m, 6H, $2CH_2$ + CH_2O epox.), 3.20–3.45 (m, 1H, OCH epox.), 3.89 (s, 3H, OCH_3), 4.02–4.20 and 4.34–4.44 (2 m, 2H, CH_2O), 4.75–4.95 (m, 1H, CHO cyclopent.), 6.80 (s, 1H Ar), 7.12 (s, 1H Ar). Anal calcd ($C_{18}H_{23}NO_4$,) C, H, N.

*4.1.16. General procedure for the synthesis of derivatives **5a** and **5b***

To oxirane **16** (0.37 g, 1.16 mmol) morpholine or 2,6-dimethylmorpholine (2 mL) was added and the mixture was heated to 50–60 °C and stirred for 18 hs. After cooling to room temperature, the reaction mixture is poured into water (50 mL), the aqueous phase was extracted with diethyl ether (3 × 20 mL); the organic phase was washed with water (2 × 20 mL), dried ($MgSO_4$) and concentrated under reduced pressure to obtain yellow oils which were purified by flash chromatography on silica gel, using as eluents firstly dethyl ether, then a mixture of diethyl ether/methanol (9:1).

*4.1.16.1. (1E)-6-(cyclopentyloxy)-5-methoxyindan-1-one O-(2-hydroxy-3-morpholin-4-ylpropyl)oxime **5a**.* Yellow solid. Mp: 84–85 °C. Yield: 100%. IR (KBr): cm^{-1} 3444 (OH). ^1H NMR ($CDCl_3$): δ 1.51–2.08 (m, 8H, $4CH_2$, cyclopent.), 2.55–2.70 and 2.83–3.02 (2 m, 10H, $2CH_2$ + CH_2N + $2CH_2N$ morph.), 3.70–3.95 (m, 7H, OCH_3 + $2CH_2O$ morph.), 4.08–4.30 (m, 3H, CHOH + CH_2O), 4.70–4.90 (m, 1H, CHO cyclopent.) 6.77 (s, 1H, Ar), 7.10 (s, 1H, Ar). ^{13}C (101 MHz, $CDCl_3$): δ 164.13, 152.17, 144.54, 139.63, 131.53, 109.35, 107.69, 81.11, 75.37, 66.79, 66.45, 60.69, 56.02, 53.96, 32.81, 28.00, 25.16, 23.45. Anal. Calcd. for ($C_{22}H_{32}N_2O_5$) C, H, N.

*4.1.16.2. (1E)-6-(cyclopentyloxy)-5-methoxyindan-1-one O-[3-(2,6-dimethylmorpholin-4-yl)-2-hydroxypropyl]oxime **5b**.* Yellow oil. Yield: 62%. IR (film): cm-^{1} 3400 (OH). ^1H NMR ($CDCl_3$): δ 1.10–1.30 (m, 6H, $2CH_3$), 1.52–2.02 (m, 8H, $4CH_2$ cyclopent.), 2.71–2.89 and 2.90–3.06 (2 m, 10H, $2CH_2$ + CH_2N + $2CH_2N$ morph.), 3.85–3.97 (m, 5H, OCH_3 + 2CHO morph.), 4.13–4.23 (m, 3H, CHOH + CH_2O), 4.75–4.90 (m, 1H, OCH cyclopent.), 6.78 (s, 1H, Ar), 7.10 (s, 1H, Ar). ^{13}C (101 MHz, $CDCl_3$): δ 164.13, 144.54, 139.63, 131.53, 109.35, 107.69, 81.11, 75.37, 70.25, 66.59, 60.59, 59.78, 56.02, 32.81, 28.00, 25.16, 23.45, 18.20. Anal. Calcd. for ($C_{24}H_{36}N_2O_5$) C, H, N.

*4.1.17. Synthesis of (1E)-6-(cyclopentyloxy)-5-methoxyindan-1-one O-[2-hydroxy-3-(-4-hydroxypiperidin-1-yl)propyl] oxime **5c***

To a solution of **16** (0.29 g, 0.91 mmol) in an. DMF (5 mL) piperidin-1-ol (0.1 g, 1 mmol) solved in an. DMF (2 mL) was added

and the mixture was heated at 60 °C and stirred for 18 hs. After cooling to room temperature, the reaction mixture was poured into water (50 mL), the aqueous phase was extracted with diethyl ether (3 × 20 mL); the organic phase was washed with water (2 × 20 mL), with brine (3 × 20 mL), dried ($MgSO_4$) and concentrated under reduced pressure to obtain a yellow oil which was purified by flash chromatography on silica gel, using as eluents firstly dethyl ether, then a mixture of diethyl ether/methanol (9:1). Yield: 33%. IR ($CHCl_3$) cm^{-1}: 3522 (OH). ^1H NMR ($CDCl_3$): δ 1.65–2.00 (m, 12H, $4CH_2$ cyclopent.+ $2CH_2$ pip.), 2.73–3.20 (m, 10H, $2CH_2 + CH_2N + 2CH_2N$ pip.), 3.81 (s, 3H, OCH_3), 3.90–4.35 (m, 4H, $CH_2O + \underline{CH}OH$ + OCH pip.), 4.70–4.82 (m, 1H, CHO cyclopent.), 5.33 (br s, 3H, OH + H_2O disappears with D_2O), 6.72 (s, 1H, Ar), 7.05 (s, 1H, Ar). ^{13}C NMR (101 MHz, $CDCl_3$) δ 164.13, 152.17, 144.54, 139.63, 131.53, 109.35, 107.69, 81.11, 75.37, 67.09, 66.41, 60.85, 56.02, 51.30, 34.69, 32.81, 28.00, 25.16, 23.45. Anal. Calcd. ($C_{23}H_{34}N_2O_5\ H_2O$) C, H, N.

4.2. NMR analysis

NMR experiments were performed at 298 K on a Bruker Avance III 400 MHz spectrometer (Milan, Italy). The NMR experiments were carried out in 500 μL of $CDCl_3$. All proton and carbon chemical shifts were assigned unambiguously using bi-dimensional experiments (COSY, NOESY and HSQC). Edited $^1H-^{13}C$ HSQC experiments were performed to confirm and follow the resonances of carbons. Phase sensitive 2D-NOESY experiments with gradient pulses in mixing time were performed with a mixing time of 700 ms in order to observe homonuclear correlation via dipolar coupling.

4.3. Biological studies

4.3.1. PDE4D catalytic domain expression and purification

The DNA fragment encoding for the catalytic domain (cat) of PDE4D (amino acids 244–578) was cloned into a pET3a vector (Merck Millipore, Darmstadt, Germany) with a C-terminal 6His-tag and transformed into *E. coli* BL21(DE3) pLysS cells (Thermo Fisher Scientific, Waltham MA, USA). Cells were cultured at 37 °C in Luria-Bertani (LB) medium supplemented with 50 mg/liter ampicillin until $OD_{600} = 0.6$. Protein expression was induced using isopropyl 1-thio-β-D-galactopyranoside (IPTG) at a final concentration of 0.5 mM and was carried out overnight at 25 °C. Cells were pelleted, resuspended in buffer A (20 mM Tris HCl pH 7.5, 150 mM NaCl), supplemented with 0.5 mM PMSF and DNase (Sigma-Aldrich), and lysed by sonication. The soluble fraction was first purified by affinity chromatography using a Ni-NTA column (Qiagen, Hilden, Germany) equilibrated with buffer A; elution was done with 400 mM imidazole. Further purification of the sample involved first a size-exclusion chromatography step using a Sephacryl 100 HR HiPrep 26/60 column (GE Healthcare, Chicago, Illinois, USA) and then an ion-exchange chromatography step using a HiPrep Q HP 16/10 column (GE Healthcare, Chicago, Illinois, USA). The final protein sample was dialyzed against buffer A and used at 10 mg/ml for crystallization experiments and at 0.025 mg/ml for inhibition assays.

4.3.2. PDE4D3 expression and purification

The PDE4D3 protein construct was expressed in baculovirus-infected insect cells. The codon-optimized PDE4D3 human sequence was synthesized by GenScript (Piscataway, NJ, USA) including two point mutations - S54D (PKA phosphomimetic) and S579A (preventing known inactivating phosphorylation [9]. The construct, bearing a C-terminal 6His-tag, was inserted in pFastBac dual vector and transformed into *E. coli* DH10EMBacY (strain kindly provided by I. Berger, University of Bristol, Bristol, UK) to generate the bacmid that was used to obtain high-titer recombinant baculovirus by PEI MAX (Polysciences Europe GmbH, Hirschberg, Germany) transfection of Sf9 at 0.8×10^6 cells/mL [31]. Expression of the protein was done in Sf9 cells infected at 1,5 × 106 cells/mL for 72h at 27 °C. Cell pellets, harvested by centrifugation, were resuspended in 50 mM Hepes pH 7.5, 500 mM NaCl, 10 mM MgCl2, 10% glycerol, 5 mM imidazole, 10 μg/mL DNaseI, 1 mM TCEP added of protease inhibitors (Roche, Mannheim, Germany) and homogenized using Emulsiflex C3 cell disruption system (Avestin). Cell lysate was cleared by centrifugation, after 5 min incubation with benzonase (Merck Millipore, Darmstadt, Germany), and the supernatant was affinity purified on Ni-NTA resin (Qiagen, Hilden, Germany). The protein fraction was eluted with 50 mM Hepes pH 7.5, 150 mM NaCl, 10% glycerol, 400 mM imidazole, 1 mM TCEP and then IEX purified on HiTrap HP Q column (GE Healthcare, Chicago, Illinois, USA) prior dilution in 100 mM Hepes pH 7.5, 10% glycerol and 1 mM DTT.

4.3.3. PDE4D activity and inhibition assays

An NADH-coupled assay was used to detect the levels of AMP resulting from cAMP hydrolysis and therefore to monitor enzyme activity [32]. Inhibition assays were carried out in 96 transparent polystyrene plates (Grainer Bio, Kremsmünster, Austria). A 132.5 μL volume of a reaction mixture containing 50 mM Tris pH 7.5, 100 mM NaCl, 10 mM $MgCl_2$, 10 mM KCl, 0.3 mM ATP, 0.6 mM PEP, 1.8 U of Pyruvate Kinase, 1.8 U of Lactate Dehydrogenase, 1.6 U Myokinase, and the enzyme was pre-incubated for 10 min at 25 °C. Then, cAMP was added to a final concentration of 0.004 mM to start the hydrolysis reaction. The oxidation of NADH to NAD^+ was monitored at 340 nm (NADH $\varepsilon_{342} = 6220\ M^{-1}cm^{-1}$) using a Spark10 M plate reader (Tecan, Männedorf, Switzerland). One unit (U) is defined as the amount of enzyme required to hydrolyze 1 μmol of cAMP to 5′-AMP per minute, while specific activity is expressed as U mg^{-1} of enzyme. Inhibition assays were carried out following the same procedure and varying the concentration of the compounds within the range 0.01 μM–300 μM. Compounds were first dissolved in 100% DMSO at 100 mM concentration and then diluted to 1% concentration in the assay buffer. IC_{50} was determined by plotting the enzyme fractional activity against the logarithm of compound concentration. Dose-response curve fitting was done using Sigma Plot (Systat Software) and Eq. (1):

$$y = \min + ((\max - \min) / (1 + 10^{(\log IC_{50} - x)})) \quad \text{(Eq. 1)}$$

where y is the fractional activity of the enzyme in the presence of inhibitor at concentration [I], max is the maximum value of y observed at [I] = 0, and min is the minimum limiting value of y at higher inhibitor concentration. All measurements were done in triplicates.

4.4. Crystallization and X-ray crystallography

Crystals of the PDE4D catalytic domain were grown by vapor diffusion using the hanging drop method. One μL of the PDE4D catalytic domain solution at 10 mg/ml concentration was mixed with 1 μL of the crystallization buffer consisting of 10–20% PEG 3350, 10–100 mM Hepes pH 7.5, 100–200 mM $MgCl_2$. The crystals thus obtained were soaked for 48h in half-concentration crystallization buffer solutions containing 1–6 mM inhibitor. Finally, crystals were flash-frozen in 20% ethylene glycol.

Diffraction data were collected at the X06DA-PXIII beamline at Swiss Light Source, Paul Scherrer Institute, Villigen, Switzerland using a wavelength of 1 Å. Diffractions images were processed using XDS and the crystal structures were solved by molecular replacement using the crystal structure of the PDE4D catalytic

domain (PDB code: 2PW3) as the search probe. All the refinements were carried out with Phenix [33]. Crystallographic data are reported in Table 3.

Accession codes

The final crystallographic coordinates of the crystal structure shown here are available as PDB entry 7AY6 and 7B9H.

Declaration of competing interest

The authors declare that they have no known competing financial interests or personal relationships that could have appeared to influence the work reported in this paper.

Acknowledgements

The authors wish to thank the X06DA-PXIII beamline personnel of the Paul Scherrer Institute, Villigen, Switzerland, for help with data collection.

Appendix A. Supplementary data

Supplementary data to this article can be found online at https://doi.org/10.1016/j.ejmech.2021.113638.

References

[1] E.R. Kandel, The molecular biology of memory: cAMP, PKA, CRE, CREB-1, CREB-2, and CPEB, Mol. Brain 5 (2012) 14, https://doi.org/10.1186/1756-6606-5-14.
[2] M.D. Houslay, P. Schafer, K.Y. Zhang, Phosphodiesterase-4 as a therapeutic target, Drug Discov. Today 10 (2005) 1503–1519, https://doi.org/10.1016/S1359-6446(05)03622-6.
[3] J. Prickaerts, P.R.A. Heckman, A. Blokland, Investigational phosphodiesterase inhibitors in phase I and phase II clinical trials for Alzheimer's disease, Expet Opin. Invest. Drugs 26 (2017) 1033–1048, https://doi.org/10.1080/13543784.2017.1364360.
[4] C. Zhang, Y. Xu, H.T. Zhang, M.E. Gurney, J.M. O'Donnell, Comparison of the pharmacological profiles of selective PDE4B and PDE4D inhibitors in the central nervous system, Sci. Rep. 7 (2017) 40115, https://doi.org/10.1038/srep40115.
[5] M.E. Gurney, E.C. D'Amato, A.B. Burgin, Phosphodiesterase-4 (PDE4) molecular pharmacology and Alzheimer's disease, Neurotherapeutics 12 (2014) 49–56, https://doi.org/10.1007/s13311-014-0309-7.
[6] D.C. Lynch, D.A. Dyment, L. Huang, S.M. Nikkel, D. Lacombe, P.M. Campeau, B. Lee, C.A. Bacino, J.L. Michaud, F.P. Bernier, J.S. Parboosingh, A.M. Innes, Identification of novel mutations confirms PDE4D as a major gene causing acrodysostosis, Hum. Mutat. 34 (2013) 97–102, https://doi.org/10.1002/humu.22222.
[7] C. Silve Acrodysostosis, A new form of pseudohypoparathyroidism? Ann. Endocrinol. 76 (2015) 110–112, https://doi.org/10.1016/j.ando.2015.03.004.
[8] O. Bruno, R. Ricciarelli, J. Prickaerts, L. Parker, E. Fedele, PDE4D inhibitors: a potential strategy for the treatment of memory impairment? Neuropharmacology 85 (2014) 290–292, https://doi.org/10.1016/j.neuropharm.2014.05.038.
[9] A.B. Burgin, O.T. Magnusson, J. Singh, P. Witte, B.L. Staker, J.M. Bjornsson, M. Thorsteinsdottir, S. Hrafnsdottir, T. Hagen, A.S. Kiselyov, L.J. Stewart, M.E. Gurney, Design of phosphodiesterase 4D (PDE4D) allosteric modulators for enhancing cognition with improved safety, Nat. Biotechnol. 28 (2010) 63–70, https://doi.org/10.1038/nbt.1598.
[10] D. Fox, A.B. Burgin, M.E. Gurney, Structural basis for the design of selective phosphodiesterase 4B inhibitors, Cell. Signal. 26 (2014) 657–663, https://doi.org/10.1016/j.cellsig.2013.12.003.
[11] C. Brullo, M. Massa, C. Villa, R. Ricciarelli, D. Rivera, M.A. Pronzato, E. Fedele, E. Barocelli, S. Bertoni, L. Flammini, O. Bruno Synthesis, Biological activities and pharmacokinetic properties of new fluorinated derivatives of selective PDE4D inhibitors, BMC (Biomed. Chromatogr.) 23 (2015) 3426–3435, https://doi.org/10.1016/j.bmc.2015.04.027.
[12] O. Bruno, A. Romussi, A. Spallarossa, C. Brullo, S. Schenone, F. Bondavalli, N. Vanthuyne, C. Roussel, New selective phosphodiesterase 4D inhibitors differently acting on long, short, and supershort isoforms, J. Med. Chem. 52 (2009) 6546–6557, https://doi.org/10.1021/jm900977c.
[13] C. Brullo, R. Ricciarelli, J. Prickaerts, O. Arancio, M. Massa, C. Rotolo, A. Romussi, C. Rebosio, B. Marengo, M.A. Pronzato, B.T. Van Hagen, N.P. Van Goethem, P. D'Ursi, A. Orro, L. Milanesi, S. Guariento, E. Cichero, P. Fossa, E. Fedele, O. Bruno, New insights into selective PDE4D inhibitors: 3-(Cyclopentyloxy)-4-methoxybenzaldehyde *O*-(2-(2,6-dimethylmorpholino)-2-oxoethyl) oxime (GEBR-7b) structural development and promising activities to restore memory impairment, Eur. J. Med. Chem. 124 (2016) 82–102, https://doi.org/10.1016/j.ejmech.2016.08.018.
[14] R. Ricciarelli, C. Brullo, J. Prickaerts, O. Arancio, C. Villa, C. Rebosio, E. Calcagno, M. Balbi, B.T.J. van Hagen, E.K. Argyrousi, M.A. Pronzato, O. Bruno, E. Fedele, Memory-enhancing effects of GEBR-32a, a new PDE4D inhibitor holding promise for the treatment of Alzheimer's disease, Sci. Rep. 7 (2017) 1–14, https://doi.org/10.1038/srep46320.
[15] O. Bruno, E. Fedele, J. Prickaerts, L.A. Parker, E. Canepa, C. Brullo, A. Cavallero, E. Gardella, A. Balbi, C. Domenicotti, E. Bollen, H.J.M. Gijselaers, T. Vanmierlo, K. Erb, C.L. Limebeer, F. Argellati, U.M. Marinari, M.A. Pronzato, R. Ricciarelli, GEBR-7b, a novel PDE4D selective inhibitor that improves memory in rodents at non-emetic doses, Br. J. Pharm. 164 (2011) 2054–2063, https://doi.org/10.1111/j.1476-5381.2011.01524.x.
[16] T. Prosdocimi, L. Mollica, S. Donini, M.S. Semrau, A.P. Lucarelli, E. Aiolfi, A. Cavalli, P. Storici, S. Alfei, C. Brullo, O. Bruno, E. Parisini, Molecular bases of PDE4D inhibition by memory-enhancing GEBR library compounds, Biochemistry 57 (2018) 2876–2888, https://doi.org/10.1021/acs.biochem.8b00288.
[17] V. Cavalloro, K. Russo, V. Vasile, L. Pignataro, A. Torretta, S. Donini, M.S. Semrau, P. Storici, D. Rossi, F. Rapetti, C. Brullo, E. Parisini, O. Bruno, S. Collina, Insight into GEBR-32a: chiral resolution, absolute configuration and enantiopreference in PDE4D inhibition, Molecules 25 (2020) 935, https://doi.org/10.3390/molecules25040935.
[18] E.J. Barreiro, A.E. Kümmerle, C.A.M. Fraga, The methylation effect in medicinal chemistry, Chem. Rev. 111 (2011) 5215–5246, https://doi.org/10.1021/cr200060g.
[19] M.J. Ashton, D.C. Cook, G. Fenton, J.A. Karlsson, M.N. Palfreyman, D. Raeburn, A.J. Ratcliffe, J.E. Souness, S. Thurairatnam, N. Vicker, Selective type IV phosphodiesterase inhibitors as antiasthmatic agents. The syntheses and biological activities of 3-(cyclopentyloxy)-4-methoxybenzamides and analogues, J. Med. Chem. 37 (1994) 1696–1703, https://doi.org/10.1021/jm00037a021.
[20] A.S. Paraskar, A. Sudalai, Enantioselective synthesis of (-)-cytoxazone and (+)-epi-cytoxazone, novel cytokine modulators via Sharpless asymmetric epoxidation and l-proline catalyzed Mannich reaction, Tetrahedron 62 (2006) 5756–5762, https://doi.org/10.1016/j.tet.2006.03.079.
[21] K. Euikyung, C. Hyung-Ok, J. Sung-Hak, K. Jong Hoon, L. Jae-Mok, S. Byung-Chul, X.X. Myung, K.R. Chung, Improvement of therapeutic index of phosphodiesterase type IV inhibitors as anti-asthmatics, BMCL 13 (2003) 2355–2358, https://doi.org/10.1016/s0960-894x(03)00405-0.
[22] E.J.E. Freyne, G.S.M. Diels, G.J.I. Andres, G.F.J. Fernandez, 1,3-Dihydro-1-(phenylalkyl)-2H-imidazole-2-one Derivatives Having PDE IV and Cytokine Activity, PCT Int. Appl., 1996. WO 9631485.
[23] L.J. Lombardo, Preparation of oxime carbamates and oxime carbonates as bronchodilators and antiinflammatory agents, Eur. Pat. Appl. (1992) 470805.
[24] B.R. Kim, G.H. Sung, J.J. Kim, Y.J. Yoon, A development of rapid, practical and selective process for preparation of Z-oximes, J. Kor. Chem. Soc. 57 (2013) 295–299, https://doi.org/10.5012/jkcs.2013.57.2.295.
[25] M. Tada, H. Hirano, A. Suzuki, Photochemistry of host-guest complex III. Effect of guest cation of the photoreactivity of acetophenone oxime derivatives having crown ether moiety, Chem. Soc. Jpn. 53 (1980) 2304–2308, https://doi.org/10.1246/bcsj.53.2304.
[26] T. Rafiq, J.L. Sorensen, Synthesis of Actinomycetes natural products JBIR-94, JBIR-125, and related analogues, Tetrahedron Lett. 56 (2015) 7108–7111, https://doi.org/10.1016/j.tetlet.2015.11.020.
[27] F.C. Meng, F. Mao, W.J. Shan, F. Qin, L. Huang, X.S. Li, Design, synthesis, and evaluation of indanone derivatives as acetylcholinesterase inhibitors and metal-chelating agents, BMCL 22 (2012) 4462–4466, https://doi.org/10.1016/j.bmcl.2012.04.029.
[28] H. Irie, S. Tanaka, Y. Zhang, J. Koyama, T. Taga, K. Machida, Synthesis of methoxyonchine and use of ^{1}H- and ^{13}C-nuclear magnetic resonance spectra for structure determination of geometrical isomers of indan-1-one oxime derivatives, Chem. Pharm. Bull. 36 (1988) 3134–3137, https://doi.org/10.1248/cpb.36.3134.
[29] The PyMOL Molecular Graphics System, Schrödinger, LLC, Portland, OR.
[30] L. Huang, H. Miao, Y. Sun, F. Meng, X. Li, Discovery of indanone derivatives as multi-target-directed ligands against Alzheimer's disease, Eur. J. Med. Chem. 87 (2014) 429–443, https://doi.org/10.1016/j.ejmech.2014.09.081.
[31] C. Bieniossek, T. Imasaki, Y. Takagi, I. Berger MultiBac, Expanding the research toolbox for multiprotein complexes, Trends Biochem. Sci. 37 (2012) 49–57, https://doi.org/10.1016/j.tibs.2011.10.005.
[32] S.P. Chock, C.Y. Huang, An optimized continuous assay for cAMP phosphodiesterase and calmodulin, Anal. Biochem. 138 (1984) 34–43, https://doi.org/10.1016/0003-2697(84)90765-6.
[33] P.D. Adams, P.V. Afonine, G. Bunkoczi, V.B. Chen, I.W. Davis N. Echols, J.J. Headd, L.W. Hung, G.J. Kapral, R.W. Grosse-Kunstleve, A.J. McCoy, N.W. Moriarty, R. Oeffner, R.J. Read, D.C. Richardson, J.S. Richardson, T.C. Terwilliger, P.H. Zwart, PHENIX: a comprehensive Python-based system for macromolecular structure solution, Acta Crystallogr. Sect. D Biol. Crystallogr. 66 (2010) 213–221, https://doi.org/10.1107/S0907444909052925.